Longitudinal correlation of the triangular flow event plane in a hybrid approach with hadron and parton cascade initial conditions

Hannah Petersen, Vivek Bhattacharya, and Steffen A. Bass
Department of Physics, Duke University, Durham, North Carolina 27708-0305, United States

Carsten Greiner
Institut für theoretische Physik, Johann Wolfgang Goethe-Universität, Max-von-Laue Strasse 1, D-60438 Frankfurt am Main, Germany
(Received 4 May 2011; revised manuscript received 2 September 2011; published 14 November 2011)

The longitudinal long-range correlations of the triangular flow event-plane angles are calculated in a Boltzmann + hydrodynamics hybrid approach. The potential to disentangle different energy deposition scenarios is explored by utilizing two different transport approaches for the early nonequilibrium evolution. In the hadronic transport approach the particle production in high-energy heavy ion reactions is mainly governed by string excitation and fragmentation processes which are absent in the parton cascade approach. We find that in both approaches the initial state shows a strong longitudinal correlation of the event-plane angles which is diluted but still persists in the final state momentum space distributions of the produced particles. The observation of this effect is an important prerequisite for the experimental determination of odd harmonics that relies on a rapidity independent event-plane definition.

DOI: 10.1103/PhysRevC.84.054908 PACS number(s): 25.75.−q, 24.10.Lx, 24.10.Nz

I. INTRODUCTION

Long-range rapidity correlations have been measured in heavy ion reactions at the Relativistic Heavy Ion Collider (RHIC) [1–5]. In two-particle correlations with a high p_T trigger hadron in the two-dimensional $\Delta\eta$-$\Delta\phi$ plane a ridge-like structure around $\Delta\phi = 0$ that extends over several units in pseudorapidity difference was observed. Later on the same phenomenon was also found in untriggered correlation functions and more detailed measurements with respect to particle composition and effective temperatures were performed that indicated the "bulk"-like properties of the ridge. Therefore the original interpretation as a jet-medium effect [6–8] has been questioned and other explanations such as Color-Glass-Condensate (CGC) inspired flux tube structures that get boosted by radial flow have become more favored [9–13].

Recently, initial state fluctuations were proposed as the major source for many of the structures that appear in two-particle correlations [14–17]. Specifically, the third Fourier coefficient of the azimuthal distribution of the final state hadrons in momentum space, namely triangular flow, was studied with great interest [18–20]. This new flow observable is directly related to the fluctuations in the initial state and is absent in hydrodynamic calculations assuming smooth initial state profiles. Triangular flow is therefore independent of the collision centrality and very sensitive to the viscosity of the produced matter [21–24].

Even though a lot of progress has been made in the study of initial conditions, in particular regarding their fluctuations, it has been rather difficult to find an observable that is directly related to the mechanism of the initial energy deposition. Long-range rapidity correlations seem to be perfectly suited for this purpose since they need to be built up very early during the evolution of the reaction due to causality. To study the effect of initial state fluctuations one needs to simulate the entire three-dimensional dynamical evolution event by event, which is computationally very expensive and makes it difficult to study two-dimensional two-particle correlations in detail.

In this paper we propose a new observable that directly quantifies the longitudinal long-range correlation of triangular flow and explore it utilizing a state-of-the-art $(3 + 1)d$ Boltzmann + hydrodynamics approach [25]. In Ref. [18] the pseudorapidity dependence of triangular flow in the hybrid approach has been published. The flatness over a broad range of pseudorapidities indicates long-range correlations, but does not actually prove that correlation. The preferred axis of the triangular shape could randomly fluctuate from one rapidity bin to the other and one would still observe a flat rapidity dependence as long as the magnitude of the third Fourier coefficient is the same in every bin. To really study the long-range correlation between the "hot spots" we propose to investigate the triangular flow event plane in different rapidity bins separately and calculate the correlation between these and the overall event plane that is reconstructed from the full phase-space information. This observable has the great advantage that it is computationally less intensive than two-particle correlations and contains similar information.

II. HYBRID APPROACH WITH HADRON AND PARTON CASCADE INITIAL CONDITIONS

In the following, we will explore this observable by using two different transport approaches to generate the initial conditions for the ideal hydrodynamic evolution to study its sensitivity to the energy deposition scenario. Let us first describe the two different approaches for the initial conditions in more detail. The initial conditions are either generated using hadron-string dynamics from the Ultrarelativistic Quantum Molecular Dynamics (UrQMD) approach [26,27] or by using a parton cascade approach (PCM) [28,29]. For the hadron-string dynamics, the initial binary nucleon-nucleon collisions are

modeled in UrQMD [26,27,30] following the Lund model of nucleon-nucleon reactions [31] involving color flux tubes excitation and fragmentation processes that provide long-range rapidity correlations and fluctuations in the energy deposition in the transverse plane. The other option is to decompose the incoming nuclei according to parton distribution functions into quarks and gluons and use a parton cascade approach to simulate the early nonequilibrium evolution [28,29,32,33]. In this case, the cross-sections for $2 \rightarrow 2$ collisions and $1 \rightarrow 2$ splittings are given by perturbative QCD calculations. We have chosen this approach since at first glance it does not contain any obvious mechanism to generate long-range correlations and thus provides a baseline for comparison. However, as we shall later see, the presence of radiated parton showers generated after the initial hard parton-parton scatterings is capable of generating long-range rapidity correlations.

For Au + Au collisions at the highest RHIC energies the starting time for the hydrodynamic evolution has been chosen to be $t_{\text{start}} = 0.5$ fm to fit the final state pion multiplicity at midrapidity. Only the matter around midrapidity ($|y| < 2$) is considered to be locally thermalized and takes part in the ideal hydrodynamic evolution. To map the point particles from the hadron/parton cascade initial state to energy, momentum, and net baryon density distributions each particle is represented by a three-dimensional Gaussian distribution [34]. The width of the Gaussian distribution has been chosen to be $\sigma = 1$ fm for UrQMD and $\sigma = 0.5$ fm for the PCM.

The ideal hydrodynamic evolution [35,36] for the hot and dense stages of the collision translates the initial fluctuations in the transverse energy density to momentum space distributions. A hadron gas equation of state [37] was used for the calculation with UrQMD initial conditions.

The transition from the hydrodynamic evolution to the transport approach when the matter is diluted in the late stage is treated as a gradual transition on an approximated constant proper time hypersurface (see Ref. [38] for details). For the hadronic calculation an energy density of 713 MeV/fm^3 was chosen as a transition criterion. Late stage hadronic rescattering and resonance decays are taken into account in the hadronic cascade.

The above event-by-event setup includes all the main ingredients that are necessary for the buildup of triangular flow [18]. Since the complete final state particle distributions are calculated, an analysis similar to that applied by experimentalists is used.

III. INITIAL STATE EVENT-PLANE CORRELATIONS

In the initial state coordinate space distributions, one can define the event-plane angles for different harmonics (we will concentrate on $n = 2$ and $n = 3$ in this analysis) in the following way:

$$\Phi_n = \frac{1}{n}\arctan\frac{\langle r^n \sin(n\phi)\rangle}{\langle r^n \cos(n\phi)\rangle}, \tag{1}$$

where r and ϕ are the polar coordinates of the particles in the center-of-mass frame of the collision. For elliptic flow this angle is the one that defines the so-called participant plane. With the used conventions Φ_n is defined in the region between $-\pi/n$ and $+\pi/n$. To explore the longitudinal correlations, the event-plane angle is calculated once in the whole rapidity range from $-2 < y < 2$ and then in different bins of width $|\Delta y| < 0.5$ separately. The distributions of the difference between those two angles in different rapidity slices is shown

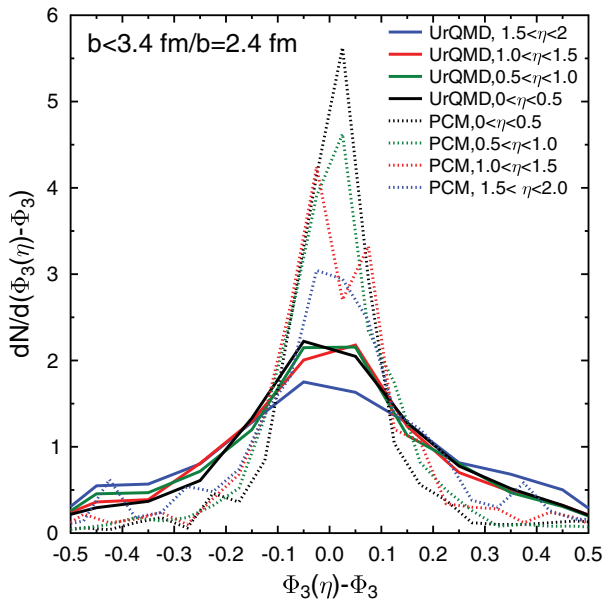

FIG. 1. (Color online) Distribution of the differences of the coordinate space event-plane angles Φ_3 in different rapidity slices in UrQMD (full line) and PCM (dotted line) initial conditions for central ($b < 3.4$ fm/$b = 2.4$ fm) Au + Au collisions at $\sqrt{s_{\text{NN}}} = 200$ GeV.

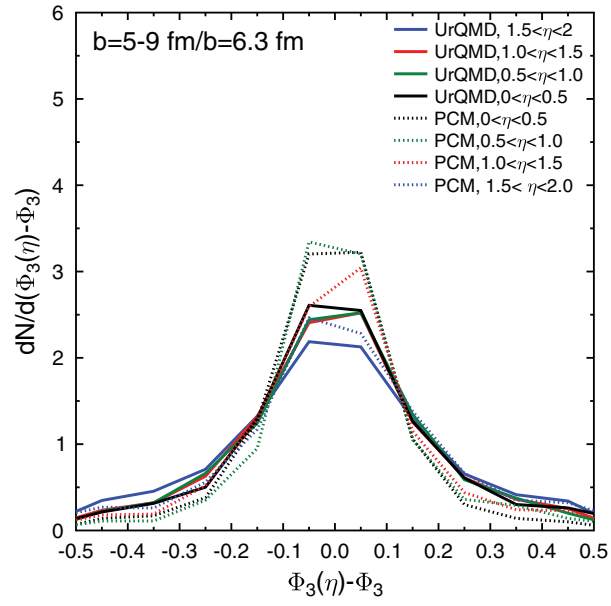

FIG. 2. (Color online) Distribution of the differences of the coordinate space event-plane angles Φ_3 in different rapidity slices in UrQMD (full line) and PCM (dotted line) initial conditions for midcentral ($b = 5$–9 fm/$b = 6.3$ fm) Au + Au collisions at $\sqrt{s_{\text{NN}}} = 200$ GeV.

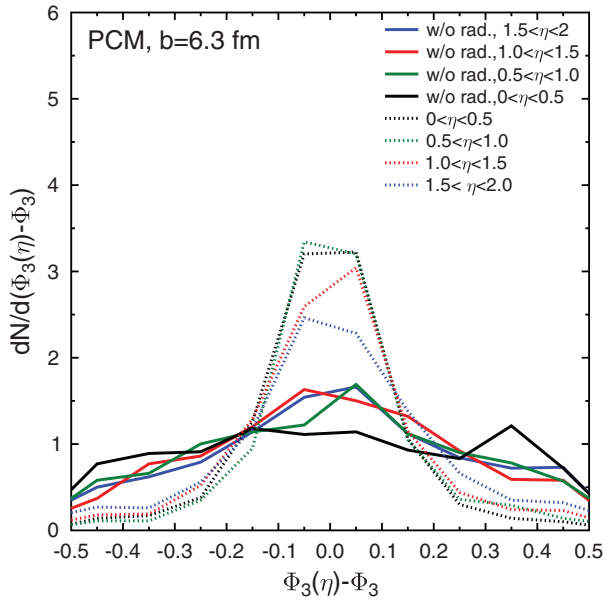

FIG. 3. (Color online) Distribution of the differences of the coordinate space event-plane angles Φ_3 in different rapidity slices from the parton cascade in the default scenario (dotted line) and without gluon radiation (full line) initial conditions for midcentral ($b = 6.3$ fm) Au + Au collisions at $\sqrt{s_{\rm NN}} = 200$ GeV.

in Fig. 1. We checked that the results are symmetric around midrapidity and the results are qualitatively unchanged if the bin size is varied from $|\Delta y| < 0.25$–1.0. Furthermore, the result without any additional physics mechanism that introduces a long-range correlation is a flat distribution (corresponding to a δ function in the $dN/d\Delta y$ distribution) that we can reproduce by sampling particles from different events together and apply the exact same correlation analysis, similar to a mixed event technique. The rapidity range over which we performed our analysis corresponds to a maximum Δy of four units.

In Figs. 1 and 2 the correlation of the event-plane angles is shown for two different centralities and the two different initial state transport approaches. In both cases, there is a strong correlation visible that is largest at midrapidity and smaller at the most forward y bin. In the parton cascade approach the longitudinal correlation can be attributed to the emission of parton showers that appear to be correlated to the preceding hard collision and are emitted along the beam axis, whereas in the hadronic transport approach the string excitation and fragmentation mechanism offers the most plausible explanation.

Figure 3 shows a comparison for the parton cascade initial conditions with and without time-like branchings, which initiate the parton showers. Without gluon emission after the hard collision, the longitudinal correlation of the triangular flow event-plane angle in the initial state is much smaller (if existent at all). That proves that the initial long-range correlation in the parton cascade is mainly caused by this associated gluon radiation. Please note that this finding is qualitatively different from the previously invoked jet-medium interactions that could lead to a ridge-like structure. The longitudinal correlations of the energy deposition in the parton cascade are generated before the medium is formed. The initial state features will then be further propagated in the hydrodynamic evolution. Therefore, the corresponding final state ridge structure will have the expected features (e.g., similar momentum distributions as the bulk particles).

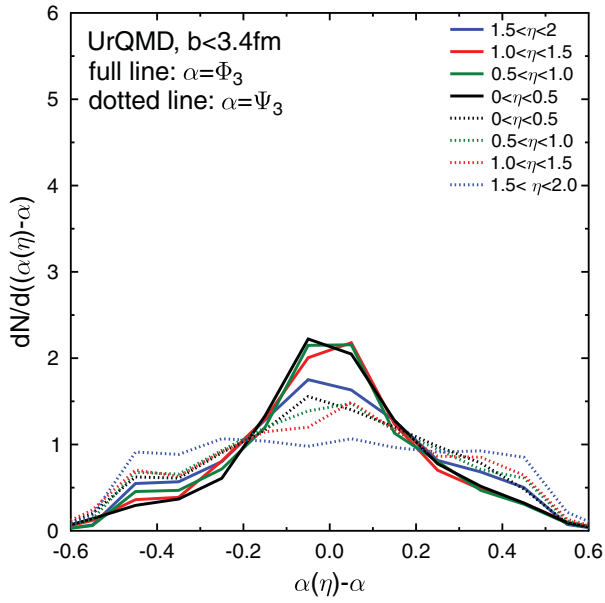

FIG. 4. (Color online) Distribution of the differences of the final momentum space (dotted line) versus initial coordinate space (full line) event-plane angles Φ_3 in different rapidity slices in the hybrid approach based on UrQMD initial conditions for central ($b < 3.4$ fm) Au + Au collisions at $\sqrt{s_{\rm NN}} = 200$ GeV.

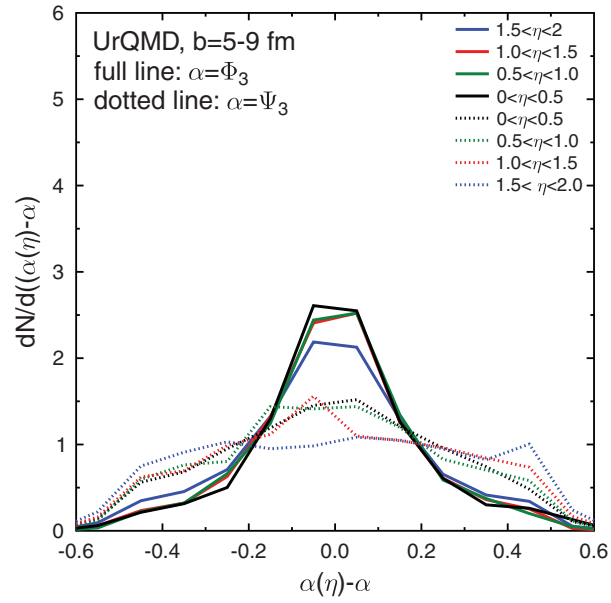

FIG. 5. (Color online) Distribution of the differences of the final momentum space (dotted line) versus coordinate space (full line) event-plane angles Φ_3 in different rapidity slices in the hybrid approach based on UrQMD initial conditions for midcentral ($b =$ 5–9 fm) Au + Au collisions at $\sqrt{s_{\rm NN}} = 200$ GeV.

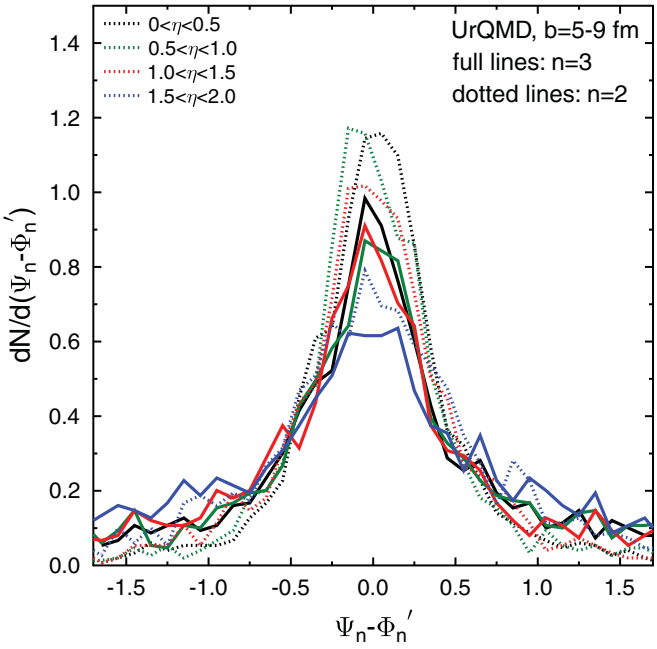

FIG. 6. (Color online) Event-by-event correlation between initial and final state event-plane angles for elliptic (dotted line) and triangular flow (full line) in different rapidity slices in the hybrid approach based on UrQMD initial conditions for midcentral (b = 5–9 fm) Au + Au collisions at $\sqrt{s_{\rm NN}} = 200$ GeV.

IV. FINAL STATE EVENT PLANE CORRELATIONS

To investigate if the initial long-range correlation survives the hydrodynamic expansion the same analysis can be performed for the final state momentum space event-plane angles

$$\Psi_n = \frac{1}{n}\arctan\frac{\langle p_T \sin(n\phi_p)\rangle}{\langle p_T \cos(n\phi_p)\rangle}, \qquad (2)$$

where (p_T, ϕ_p) are polar coordinates in momentum space. In Figs. 4 and 5 the longitudinal correlation of the final state event-plane angles Ψ_3 is shown in comparison to the previously presented distribution for Φ_3. The correlation gets significantly diluted during the ideal hydrodynamic expansion, but it persists also in the final state particle distribution with the exception of the most forward/backward rapidity bin that is accessible in this calculation. We checked that the same result qualitatively is obtained by employing the parton cascade initial conditions. The final state event-plane angles Ψ_3 in different rapidity bins can be measured in the experiment to investigate the longitudinal correlations of triangular flow and to legitimate the assumption that the event-plane angle does not change as a function of rapidity.

Another way to study the initial and final state correlations of the event-plane angles is shown in Fig. 6. Here the differences between the two angles in different rapidity bins are shown for midcentral collisions in the hybrid approach based on UrQMD initial conditions. As a comparison the correlation for elliptic flow at is also shown. For the three rapidity bins between 0 and 1.5 the correlation is clearly visible for triangular flow as well, whereas it is less pronounced in the most forward/backward bin. This confirms the conclusion of Fig. 5 that the long-range correlation only survives over three units in rapidity around $y = 0$.

V. SUMMARY AND CONCLUSION

In summary, we proposed a new way to investigate the long-range correlations of triangular flow in heavy ion collisions. A hadron and a parton cascade approach both lead to sizable long-range correlations in the initial state. These correlations are translated to the final state hadron distributions, but are significantly diluted and smoothed out during the final hadronic rescattering. Measuring the triangular flow event-plane angles in different rapidity bins serves as a prerequisite to legitimate the assumption of a constant event plane over rapidity as it is commonly assumed by experimental groups. The second conclusion is that one needs to take into account a realistic dynamical evolution (e.g., Refs. [39,40]) to prove that the long-range correlations that might be initially established also survive to the final state particle distributions instead of simple parametrizations.

ACKNOWLEDGMENTS

We are grateful to the Open Science Grid for the computing resources. The authors thank Dirk Rischke for providing the 1 fluid hydrodynamics code. This work was supported by the Hessian LOEWE initiative through the Helmholtz International Center for FAIR (HIC for FAIR). H.P. acknowledges support by the Feodor Lynen program of the Alexander von Humboldt foundation. This work was supported in part by US Department of Energy Grant No. DE-FG02-05ER41367 and NSF Grant No. PHY-09-41373. The authors thank G. Qin, R. Snellings, N. Xu, and Z. Xu for fruitful discussions.

[1] J. Adams *et al.* (STAR Collaboration), Phys. Rev. Lett. **95**, 152301 (2005).
[2] J. Adams *et al.* (STAR Collaboration), Phys. Rev. C **73**, 064907 (2006).
[3] J. Putschke, J. Phys. G **34**, S679 (2007).
[4] B. I. Abelev *et al.* (STAR Collaboration), Phys. Rev. C **80**, 064912 (2009).
[5] B. Alver *et al.* (PHOBOS Collaboration), Phys. Rev. Lett. **104**, 062301 (2010).
[6] A. Majumder, B. Muller, and S. A. Bass, Phys. Rev. Lett. **99**, 042301 (2007).
[7] E. V. Shuryak, Phys. Rev. C **76**, 047901 (2007).
[8] C. Y. Wong, Phys. Rev. C **78**, 064905 (2008).
[9] A. Dumitru, F. Gelis, L. McLerran, and R. Venugopalan, Nucl. Phys. A **810**, 91 (2008).
[10] S. Gavin, L. McLerran, and G. Moschelli, Phys. Rev. C **79**, 051902 (2009).
[11] K. Dusling, F. Gelis, T. Lappi, and R. Venugopalan, Nucl. Phys. A **836**, 159 (2010).
[12] G. Moschelli and S. Gavin, Nucl. Phys. A **836**, 43 (2010).

[13] G. Moschelli and S. Gavin, arXiv:0911.0094.
[14] B. Alver and G. Roland, Phys. Rev. C **81**, 054905 (2010); **82**, 039903(E) (2010).
[15] M. Luzum, Phys. Lett. B **696**, 499 (2011).
[16] Y. Hama, R. P. G. Andrade, F. Grassi, and W. L. Qian, Nonlin. Phenom. Complex Syst. **12**, 466 (2009).
[17] P. Sorensen, B. Bolliet, A. Mocsy, Y. Pandit, and N. Pruthi, arXiv:1102.1403.
[18] H. Petersen, G. Y. Qin, S. A. Bass, and B. Muller, Phys. Rev. C **82**, 041901 (2010).
[19] G. Y. Qin, H. Petersen, S. A. Bass, and B. Muller, Phys. Rev. C **82**, 064903 (2010).
[20] G. L. Ma and X. N. Wang, Phys. Rev. Lett. **106**, 162301 (2011).
[21] B. H. Alver, C. Gombeaud, M. Luzum, and J. Y. Ollitrault, Phys. Rev. C **82**, 034913 (2010).
[22] B. Schenke, S. Jeon, and C. Gale, Phys. Rev. Lett. **106**, 042301 (2011).
[23] B. Schenke, S. Jeon, and C. Gale, Phys. Lett. B **702**, 59 (2011).
[24] D. Teaney and L. Yan, Phys. Rev. C **83**, 064904 (2011).
[25] H. Petersen, J. Steinheimer, G. Burau, M. Bleicher, and H. Stocker, Phys. Rev. C **78**, 044901 (2008).
[26] S. A. Bass *et al*., Prog. Part. Nucl. Phys. **41**, 255 (1998); **41**, 225 (1998).
[27] M. Bleicher *et al*., J. Phys. G **25**, 1859 (1999).
[28] K. Geiger, Phys. Rep. **258**, 237 (1995).
[29] S. A. Bass, B. Muller, and D. K. Srivastava, Phys. Lett. B **551**, 277 (2003).
[30] H. Petersen, M. Bleicher, S. A. Bass, and H. Stocker, arXiv:0805.0567.
[31] B. Andersson, G. Gustafson, G. Ingelman, and T. Sjostrand, Phys. Rep. **97**, 31 (1983).
[32] K. Geiger and B. Muller, Nucl. Phys. B **369**, 600 (1992).
[33] K. Geiger, Comput. Phys. Commun. **104**, 70 (1997).
[34] J. Steinheimer, M. Bleicher, H. Petersen, S. Schramm, H. Stocker, and D. Zschiesche, Phys. Rev. C **77**, 034901 (2008).
[35] D. H. Rischke, S. Bernard, and J. A. Maruhn, Nucl. Phys. A **595**, 346 (1995).
[36] D. H. Rischke, Y. Pursun, and J. A. Maruhn, Nucl. Phys. A **595**, 383 (1995); **596**, 717(E) (1996).
[37] D. Zschiesche, S. Schramm, J. Schaffner-Bielich, H. Stoecker, and W. Greiner, Phys. Lett. B **547**, 7 (2002).
[38] Q. F. Li, J. Steinheimer, H. Petersen, M. Bleicher, and H. Stocker, Phys. Lett. B **674**, 111 (2009).
[39] Z. Xu and C. Greiner, Phys. Rev. C **71**, 064901 (2005).
[40] Z. Xu and C. Greiner, Phys. Rev. C **76**, 024911 (2007).